Combined Deep CNN–LSTM Network-based Multitasking Learning Architecture for Noninvasive Continuous Blood Pressure Estimation using Difference in ECG-PPG Features

Da Un Jeong
Kumoh National Institute of Technology
Ki Moo Lim (kmlim@kumoh.ac.kr)
Kumoh National Institute of Technology

Research Article

Keywords: pulse transit time (PTT), photoplethysmography (PPG), electrocardiogram (ECG) , diastolic blood pressures (DBP)

Posted Date: January 5th, 2021

DOI: https://doi.org/10.21203/rs.3.rs-137994/v1

Abstract

The pulse transit time (PTT), which is the difference between the R-peak time of the electrocardiogram (ECG) signal and the systolic peak of the photoplethysmography (PPG) signal, is an indicator that enables noninvasive and continuous blood pressure estimation. However, it is difficult to accurately measure the PTT from the ECG and PPG signals because they have inconsistent shapes owing to patient-specific physical characteristics, pathological conditions, and movements. Accordingly, complex preprocessing is required to estimate blood pressure based on PTT. In this paper, as an alternative solution, we propose a noninvasive continuous algorithm using the difference between the ECG and PPG as a new feature that can include PTT information. The proposed algorithm is a deep CNN–LSTM-based multitasking machine learning model that outputs simultaneous prediction results of systolic (SBP) and diastolic blood pressures (DBP). The prediction accuracies of SBP and DBP using the proposed model were 0.017±1.624 mmHg and 0.164±1.297 mmHg, respectively. This result corresponded to Grade A according to the BHS and AAMI standards, which are the validation standards for blood pressure measuring devices.

Introduction

There are two types of methods used to measure blood pressure: invasive and noninvasive. In the commonly used noninvasive method, blood pressure is measured through the pulse sound generated when the blood vessels in the forearm are compressed by injecting air into the cuff [1, 2]. However, in the case of noninvasive blood pressure (NIBP) measurement using a cuff, blood pressure cannot be continuously measured. In the invasive blood pressure measurement method, blood pressure can be measured continuously. However, it is used only for patients with acute dysfunction failures, who are in a critical condition in an intensive care unit (ICU), and the blood pressure is measured by inserting a cannula into the artery [3].

Many research groups have proposed a blood pressure measurement algorithm based on electrocardiography (ECG) and photoplethysmography (PPG) for noninvasive and continuous blood pressure measurements [4, 5]. These were developed based on the known relationship between blood pressure and pulse transit time (PTT). Therefore, blood pressure can be continuously estimated by continuously measuring changes in the PTT [6, 7]. Proença et al. expressed the relationship between PTT and blood pressure using a nonlinear equation [8], and Whong and Poon estimated the relationship between blood pressure, PTT, and heart rate through linear regression [9]. PTT can be measured through the time difference between the R-peak of the ECG and the systolic peak of the PPG; however, this difference is not easy to calibrate because it changes according to the physiological characteristics and pathological conditions of each individual. This may result in a decrease in accuracy or a problem with the reliability of estimating blood pressure for a completely new patient group rather than a verified patient group [10].

Meanwhile, several research groups have continuously estimated blood pressure using machine learning algorithms via features extracted from ECG and PPG signals. Chen et al. proposed a blood pressure estimation method using a genetic algorithm-mean influence value-support vector regression (GA-MIV-SVR). They extracted various features, including features related to PTT from ECG and PPG signals, and finally selected features to predict systolic blood pressure (SBP) and diastolic blood pressure (DBP) using mean influence value rankings. The obtained prediction performance satisfied the AAMI (Association for the Advanced of Medical Instrument protocols) standard (Error: 3.27 ± 5.52 mmHg for SBP and 1.16 ± 1.97 mmHg for DBP) [4]. Furthermore, Sharifi et al. proposed a multiadaptive regression spline (MARS) method based on ECG and PPG signals. They predicted SBP, DBP, and mean blood pressure with high predictive accuracies of -0.29 ± 9.1 mmHg, -0.09 ± 5.21 mmHg, and − 0.16 ± 4.6 mmHg, respectively [11]. Kachuee et al. extracted the heart rate, PPG features, and PTT features from ECG and PPG through feature engineering and used them to continuously estimate blood pressure, considering changes in PTT according to individual physiology [5]. They showed that DBP can be accurately estimated using a support vector machine method.

The aforementioned studies estimated blood pressure using features extracted by conducting a complex feature engineering process. In this paper, we propose an artificial neural network algorithm capable of continuously and noninvasively estimating blood pressure based on the difference between ECG and PPG signals, including information on PTT. The proposed algorithm is a combined deep CNN–LSTM network-based multitasking learning architecture model that can output the predicted results of SBP and DBP by considering the morphological features of the ECG and PPG signals, along with temporal features.

Results

The SBP and DBP used as the correct answers for supervised learning of the proposed model were 119.2 (94–147) mmHg and 70.8 (56–92) mmHg on average, respectively (Supplementary Fig. S1). We evaluated the accuracy of the blood pressure predicted by the proposed model using the determination coefficient (R^2) and the mean squared error, which are the indicators used to evaluate the performance of the regression model (Fig. 1). The predicted accuracy of SBP was higher than that of DBP; the R^2 values of the predicted SBP and the predicted DBP were 0.980 (p-value < 0.05) and 0.967 (p-value < 0.05), respectively, for the predicted DBP (Fig. 1B). Furthermore, the adjusted R^2 values were 0.979 and 0.966 for SBP and DBP, respectively. Accordingly, the mean squared errors of SBP and DBP were 2.688 mmHg and 1.79 mmHg, respectively.

Figure 2 shows the error distribution of the actual blood pressure (true value) and the predicted blood pressure to evaluate the accuracy and precision of the blood pressure predicted by the proposed model. Within the error range of ± 5 mmHg, the predicted values of SBP and DBP were 99.4% and 99.6%, respectively (Figs. 2A, 2B, and Table 1). These results corresponded to Grade A according to the British Hypertension Standard (BHS), a blood pressure monitor certification standard [12]. The precision of the estimated blood pressure was confirmed using the error histogram shown in Figs. 2C and 2D. The errors

between the estimated and target blood pressure were normally distributed at approximately 0 mmHg in both SBP and DBP. By conducting the Durbin–Watson test to verify the autocorrelation between the observed values and the predicted values of the proposed model, it was confirmed that independence of the SBP and DBP errors was satisfied (d-statics = 1.97 for SBP and 1.99 for DBP). The mean errors of SBP and DBP were 0.017 mmHg and 0.164 mmHg, respectively, and the standard deviations of the errors were 1.624 mmHg and 1.297 mmHg, respectively, which passed the AAMI standard (Table 2) [13]. The resulting 95% confidence intervals of the predicted SBP and DBP prediction errors were (-3.17 mmHg, 3.20 mmHg) and (-2.71 mmHg, 2.38 mmHg), respectively.

Table 1
BHS and AAMI standards

	Error distribution	SBP	DBP
BHS	Error distribution < 15 (95%)	100.0%	100.0%
	Error distribution < 10 (85%)	99.93%	100.0%
	Error distribution < 5 (60%)	99.44%	99.6%
AAMI standard	Mean error (< 5 mmHg)	0.017 mmHg	0.164 mmHg
	STD of error (< 7 mmHg)	1.624 mmHg	1.297 mmHg

Table 2
Prediction performance comparison

Model		Error (mmHg)		BHS standard	AAMI standard
		MAE	STD		
Chen et al. [4]	SBP	3.27	5.52	A	-
	DBP	1.16	1.97	A	-
Sharifi et al. [11]	SBP	0.29	9.1	-	-
	DBP	0.09	5.21	-	-
Kachuee et al. [5]	SBP	12.38	16.17	-	-
	DBP	6.34	8.45	B	
Proposed model	SBP	0.02	1.62	A	Pass
	DBP	0.16	1.30	A	Pass

Discussion

In this study, we developed an NIBP algorithm using a combined deep CNN–LSTM network-based multitasking learning architecture. The combined deep CNN–LSTM model was constructed based on the LSTM–CNN model of Xia et al. [14] to extract morphological and temporal features from the signal difference between ECG and PPG.

The proposed model estimated SBP and DBP using the signal difference between the ECG and PPG signals as input. The R-peak of the ECG refers to the electrical excitation time before the heart contracts [15], and the systolic peak of PPG denotes the time until the pulse caused by heart contraction reaches the peripheral end [16]. Accordingly, the difference between the ECG and PPG signals includes information on the electromechanical delay, which is the time delay of electrical excitation and mechanical contraction of the heart, as well as PTT (Supplementary Fig. S2).

The output layer of the proposed model used a linear function [17] to predict the SBP and DBP using a linear regression model. Next, the R^2 value was used to measure the degree to which the estimated linear model fits the given data. This refers to the proportion of the variation in the dependent variable that can be explained using the applied model [18]. In general, the accuracy may improve as the number of independent variables in the regression model increases, but the actual data may not be properly predicted because of overfitting to the training data [19]. Therefore, the adjusted R^2 was calculated to prevent overfitting or overestimation of the prediction accuracy of the proposed model by adding a penalty according to the effects of the added independent variables on SBP and DBP [18, 19].

The database used in this study was obtained from ICU patients who needed intensive care and continuous monitoring. Each data point may change the shape of the signal according to the patient's condition at the time of measurement, even if it is from the same patient. The combined deep CNN–LSTM architecture model can extract features, including both the continuous characteristics of the signal over time and the morphological characteristics of the input signal sequence. Accordingly, the predicted blood pressure was of high accuracy, but the error increased as the blood pressure increased (Fig. 1 and Fig. 2). This happened due to three reasons: First, because the average age group of the patients for whom the data were acquired was 65 years old. A sudden change in blood pressure was observed in elderly people, which created a reliability problem in the true blood pressure label used to train the supervised learning model. Second, the signal used included not only the patient's motion artifacts that can be removed through preprocessing but also morphological changes due to certain diseases that are difficult to remove through preprocessing. Finally, it was predicted that the proposed model could not fully learn the signal characteristics of these factors. These problems were also observed in preceding studies; however, it can be seen that the error rate obtained through our proposed model is lower than that in advanced studies (Table 2) [4, 5, 11].

Most advanced studies have trained and used individual models to predict the SBP and DBP. However, the combined deep CNN–LSTM architecture-based multitasking model developed in this study outputs both SBP and DBP simultaneously using a single model. This can lead to better performance compared to that when training separately for each factor because the common representative factors of SBP and DBP are extracted while the ECP and PPG difference signals pass through a shared layer [20, 21]. It was shown that the prediction performance of the proposed model is greater than that of the models developed in advanced studies.

The error histograms of the proposed model showed a normal distribution form, and it was statistically confirmed that the mean errors converged close to zero and satisfied the normality (Figs. 2C and 2D). In general, regression models of time-series data, such as blood pressure, may correlate with each error value [22]. This is called autocorrelation, and a regression model with autocorrelation in which the error of the predicted value of the model is affected by the error of adjacent observation values may not be completely reliable. Therefore, the Durbin–Watson test was performed to test the autocorrelation between the observed values and the predicted values of the proposed model, and it was confirmed that the independence of error was satisfied through the d-statistics adjacent to 2 for both prediction errors of SBP and DBP [22, 23].

The BHS guideline evaluates the accuracy of the sphygmomanometer's prediction of SBP in four grades from A to D according to the cumulative percentage of the predicted SBP within 5, 10, and 15 mmHg of the errors. Here, A is the most accurate, and the accuracy decreases toward D [12]. Besides, the AAMI guidelines require that the average difference between the true and predicted values should be less than 5 mmHg, and the standard deviation for 85% of the true values should be less than 8 mmHg [13]. The model proposed in this paper achieved an accuracy that satisfied both of these guidelines.

There are several limitations to our proposed model. First, the accuracy of long-term monitoring was not verified. For LSTM models, the accuracy may vary depending on the measurement time of the data used [24]. Accordingly, it is not known whether the accuracy of our proposed model decreases or increases when estimating blood pressure using long-term data from weeks to months. Second, the generalizability of the model was not verified. In this study, the data of ICU patients from PhysioNet were used. Although the signals were simultaneously measured, a missing signal or a signal of poor quality was removed from the dataset. Accordingly, the number of samples used for verification of the proposed model was 7,400, and the number of patients was 10, and thus the applicability of the model to many patients has not been verified. Therefore, if the generalizability of the model is validated through verification and correction of the model through more data, it can be applied to medical devices requiring long-term monitoring, including patient monitors and implantable cardiac devices such as the Holter ECG monitoring system.

Methods

1. Dataset

In this study, we used ECG, PPG, and atrial blood pressure (ABP) signals measured simultaneously in PhsioNet's Multi-parameter Intelligent Monitoring for Intensive Care (MIMIC) Database [25, 26]. Among the data of 57 patients (36 males and 21 females), the data that did not include ECG, PPG, and ABP, or data containing missing signals were not used. Finally, the ECG, PPG, and ABP data of 48 patients (30 males and 18 females) receiving intensive care were used for prediction, and the average age of the patients was 69.9 (21–92) years. Patients had one of 13 diseases, including bleeding, respiratory failure, congestive heart failure/pulmonary edema, brain injury, sepsis, angina, postoperative valve, postoperative coronary artery bypass graft, cord compression, trauma, renal failure, myocardial infarction, and cardiogenic shock. Each signal was acquired with a sampling frequency of 125 Hz for different recording times, but the average recording time was 42.7 (10.5–77.4) hours.

2. Preprocess

Simultaneously measured signals collected from the PhysioNet database were randomly extracted from each patient to obtain 6,000 samples (48 s). To remove motion artifacts and solve the baseline wandering problem, a bandpass filter of 2 Hz to 20 Hz was applied to the ECG signal, and a bandpass filter of 0.5 Hz to 20 Hz was applied to the PPG signal. After extracting the R-peak from the filtered ECG, R(n-1)-R(n + 1) sequences were generated from the ECG, PPG, and ABP signals based on the detected R-peak (n) of the ECG to include two cycles. Zero padding was applied based on the maximum R–R sequence to compensate for the difference in the data length of the generated R–R sequence due to the change in the R–R interval according to time.

The generated ECG and PPG sequences were transformed such that the maximum and minimum were + 1 and − 1, respectively, using the MinMax scaling technique. Next, the difference between the converted ECG and PPG signals was calculated and used as the input to the combined deep CNN–LSTM

architecture-based multitasking model. Besides, after extracting the peaks and inverse peaks from the ABP sequence, the average values of each peak were calculated and used as target values for SBP and DBP.

3. Model structures

The proposed model consisted of a shared layer to extract morphological and temporal features from the signal difference between ECG and PPG, and a specific layer to predict SBP and DBP. The shared layer consisted of one CNN layer for morphological features and three LSTM layers for temporal features. They were connected through a batch normalization layer to prevent overfitting. The CNN layer was composed of 56 kernels of size 10, and a rectified linear unit (ReLU) [27] was used as an activation function. Furthermore, L2 regularization was applied to improve the generalization performance of the proposed model. The three LSTM layers consisted of one bidirectional LSTM with 28 neurons and two unidirectional LSTMs connected to specific layers through a global average pooling layer. Each specific layer of SBP and DBP consisted of two fully connected layers and an output layer. The number of neurons in the fully connected layers was 28 and 16, respectively, and both activation functions were ReLU. Finally, we used a linear function [17] as the activation function of the output layer for SBP and DBP (Fig. 3).

4. Model train and evaluation

Eighty percent of the total dataset was used to train the model and 20% to evaluate the model performance. Furthermore, 10% of the training data was used for validation to prevent the model from overfitting the training dataset. The mean squared error was used as the error function for the output result, and Adam (Adaptive Moment Estimation) [28] with a learning rate of 0.01 and a decay rate of 0.00002 was used as the model optimization function. The model was trained 1,000 times with a batch size of 28; however, the optimal model with hyperparameters was selected as the final model through early stopping.

The accuracy of SBP and DBP predicted by the proposed model was evaluated through the root mean squared error and the mean absolute error [29], along with the value of R^2 and mean squared error [17, 18] used in the performance evaluation of the regression model. Besides, the possibility of grafting the proposed model into medical devices was verified using the BHS [12] and AAMI [13] standards, which are the blood pressure monitor certification standards [12], [13].

Declarations

Acknowledgements

This research was partially supported by the NRF (National Research Foundation) under basic engineering research project (2016R1D1A1B0101440) and the EDISON (NRF-2011-0020576) Programs, and the Grand Information Technology Research Center Program through the Institute of Information &

Communications Technology and Planning & Evaluation (IITP) funded by the Ministry of Science and ICT (MSIT), Korea (IITP-2020-2020-0-01612).

Author contributions statement

This manuscript is the intellectual product of the entire team. DUJ wrote the machine learning source code and the manuscript, performed the data analysis, and interpreted the results. KML designed the study, and reviewed and revised the whole manuscript based on the results. All authors read and approved the final manuscript.

Additional information

Data availability

In this study, publicly available datasets were used to analyze. This data can be found here: https://www.physionet.org/content/mimicdb/1.0.0/.

Competing interests

The authors declare that the research was conducted in the absence of any commercial or financial relationships that could be construed as a potential conflict of interest.

References

1. Alpert, B. S., Quinn, D. & Gallick, D. Oscillometric blood pressure: A review for clinicians. *J. Am. Soc. Hypertens.* **8**, 930–938 (2014).
2. Perloff, D., Grim, C., Flack, J. & Frohlich, E. D. Human Blood Pressure Determination by Sphygmomanometry. *Circulation* **88**, 2460–2470 (1993).
3. Gupta, B. Monitoring in the ICU Anaesthesia Update in. *Updat. Anaethesia* **28**, 37–42 (2012).
4. Chen, S., Ji, Z., Wu, H. & Xu, Y. A non-invasive continuous blood pressure estimation approach based on machine learning. *Sensors (Switzerland)* **19**, (2019).
5. Kachuee, M., Kiani, M. M., Mohammadzade, H. & Shabany, M. Cuff-less high-accuracy calibration-free blood pressure estimation using pulse transit time. *Proc. - IEEE Int. Symp. Circuits Syst.* **2015-July**, 1006–1009 (2015).
6. Geddes, L. A., Voelz, M., James, S. & Reiner, D. Pulse arrival time as a method of obtaining systolic and diastolic blood pressure indirectly. *Med. Biol. Eng. Comput.* **19**, 671–672 (1981).

7. Lokharan, M., Lokesh Kumar, K. C., Harish Kumar, V., Kayalvizhi, N. & Aryalekshmi, R. Measurement of pulse transit time (PTT) using photoplethysmography. *IFMBE Proc.* **61**, 130–134 (2017).
8. Proença, J., Muehlsteff, J., Aubert, X. & Carvalho, P. Is Pulse Transit Time a good indicator of blood pressure changes during short physical exercise in a young population? *2010 Annu. Int. Conf. IEEE Eng. Med. Biol. Soc. EMBC'10* 598–601 (2010) doi:10.1109/IEMBS.2010.5626627.
9. Wong, M. Y. M., Poon, C. C. Y. & Zhang, Y. T. An evaluation of the cuffless blood pressure estimation based on pulse transit time technique: A half year study on normotensive subjects. *Cardiovasc. Eng.* **9**, 32–38 (2009).
10. Peter, L., Noury, N. & Cerny, M. A review of methods for non-invasive and continuous blood pressure monitoring: Pulse transit time method is promising? *Irbm* **35**, 271–282 (2014).
11. Sharifi, I., Goudarzi, S. & Khodabakhshi, M. B. A novel dynamical approach in continuous cuffless blood pressure estimation based on ECG and PPG signals. *Artif. Intell. Med.* **97**, 143–151 (2019).
12. O'Brien, E. *et al.* The british hypertension society protocol for the evaluation of blood pressure measuring devices. *J. Hypertens.* **11**, 677–679 (1993).
13. White, W. B. *et al.* National standard for measurement of resting and ambulatory blood pressures with automated sphygmomanometers. *Hypertension* **21**, 504–509 (1993).
14. Xia, K., Huang, J. & Wang, H. LSTM-CNN Architecture for Human Activity Recognition. *IEEE Access* **8**, 56855–56866 (2020).
15. Dale, D. *Cardiology - Rapid Interpretation of EKG's*. (cover publishing company, 2000).
16. Elgendi, M., Norton, I., Brearley, M., Abbott, D. & Schuurmans, D. Systolic Peak Detection in Acceleration Photoplethysmograms Measured from Emergency Responders in Tropical Conditions. *PLoS One* **8**, 1–11 (2013).
17. Weisberg, S. *Applied Linear Regression*. *John Wiley & Sons* vol. 528 (2005).
18. Miles, J. R Squared, Adjusted R Squared. *Wiley StatsRef Stat. Ref. Online* 2–4 (2014) doi:10.1002/9781118445112.stat06627.
19. Cohen, J., Cohen, P., West, S. G. & Aiken, L. S. *Applied multiple regression/correlation analysis for the behavioral sciences*. (Routledge, 2013).
20. Liu, H., Cai, J. & Ong, Y. S. Remarks on multi-output Gaussian process regression. *Knowledge-Based Syst.* **144**, 102–121 (2018).
21. Borchani, H., Varando, G., Bielza, C. & Larrañaga, P. A survey on multi-output regression. *Wiley Interdiscip. Rev. Data Min. Knowl. Discov.* **5**, 216–233 (2015).
22. Dubbin, J. & Watson, G. S. Testing for serial correlation in least squares regression. II. *Biometrika* **38**, 159–178 (1951).
23. Savin, N. E. & White, K. J. The Durbin-Watson Test for Serial Correlation with Extreme Sample Sizes or Many Regressors Author (s): N . E . Savin and Kenneth J . White. *Econometrica* **45**, 1989–1996 (1977).
24. Schmidhuber, J. & Hochreiter, S. Long short-term memory. *Neural Comput.* **9**, 1735–1780 (1997).

25. Moody, G. B. & Mark, R. G. A Database to Support Development and Evaluation of Intelligent Intensive Care Monitoring. *Comput. Cardiol.* **23**, 657–660 (1996).
26. Goldberger, A. L. *et al.* PhysioBank, Physio Toolkit, and Physio Net. *Circulation* **101**, e215–e220 (2000).
27. Xavier, G., Antoine, B. & Yoshua, B. Deep sparse rectifier neural networks. in *International Conference on Artificial Intelligence and statistics (AISTATS)* vol. 15 315–323 (2011).
28. Kingma, D. P. & Ba, J. L. Adam: A method for stochastic optimization. in *3rd International Conference on Learning Representations, ICLR 2015 - Conference Track Proceedings* 1–15 (2015).
29. Willmott, C. J. & Matsuura, K. Advantages of the mean absolute error (MAE) over the root mean square error (RMSE) in assessing average model performance. *Clim. Res.* **30**, 79–82 (2005).
30. O'Brien, E., Waeber, B., Parati, G., Staessen, J. & Myers, M. G. Blood pressure measuring devices: Recommendations of the European Society of Hypertension. *Br. Med. J.* **322**, 531–536 (2001).
31. O'Brien, E. & Atkins, N. A comparison of the British Hypertension Society and Association for the Advancement of Medical Instrumentation protocols for validating blood pressure measuring devices: Can the two be reconciled? *J. Hypertens.* **12**, 1089–1094 (1994).
32. O'Brien, E. *et al.* The british hypertension society protocol for the evaluation of blood pressure measuring devices. *J. Hypertens.* **11**, 677–679 (1993).

Figures

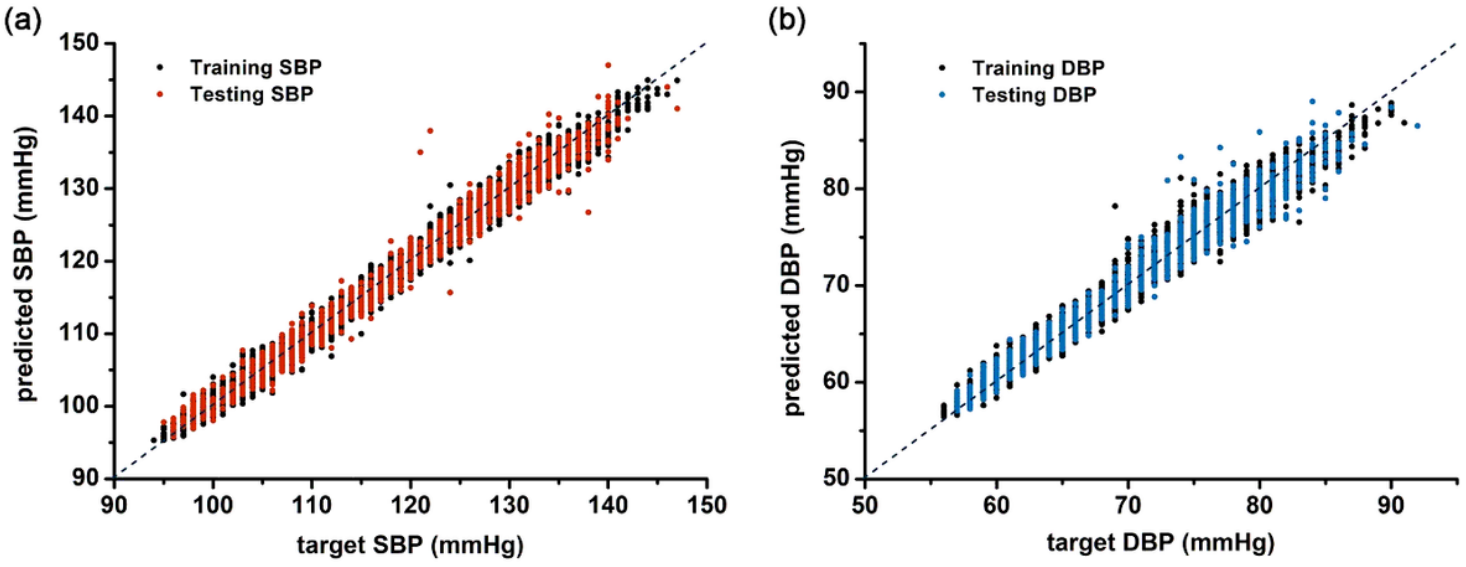

Figure 1

Prediction performance of the proposed model. (A; training and test systolic blood pressure, B; training and test diastolic blood pressure)

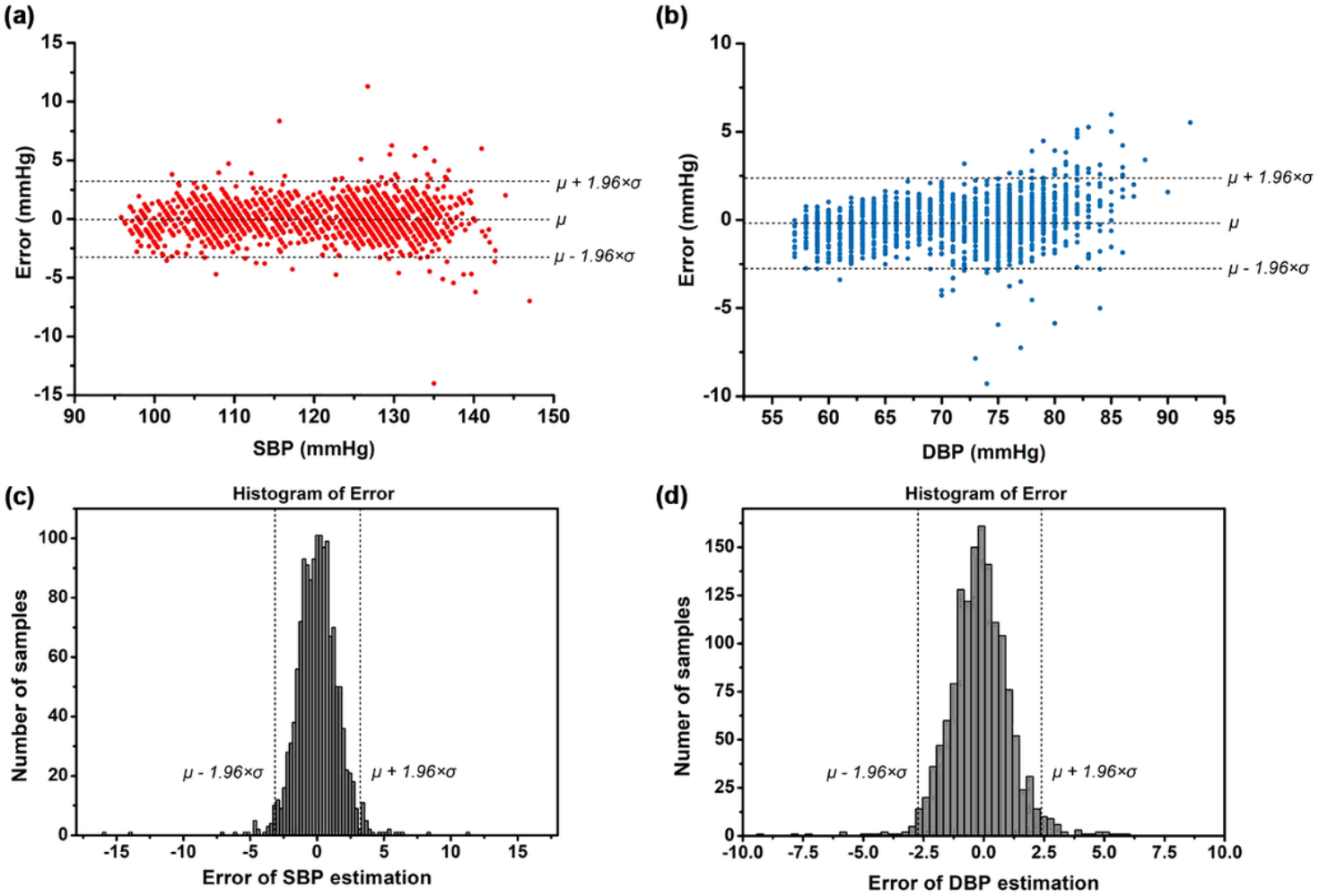

Figure 2

Error distributions of the proposed model. (A, B) Errors of predicted blood pressure over target blood pressures (A; systolic blood pressure, B; diastolic blood pressure). (C, D) Error histogram of predicted blood pressures (C; systolic blood pressure, D; diastolic blood pressures)

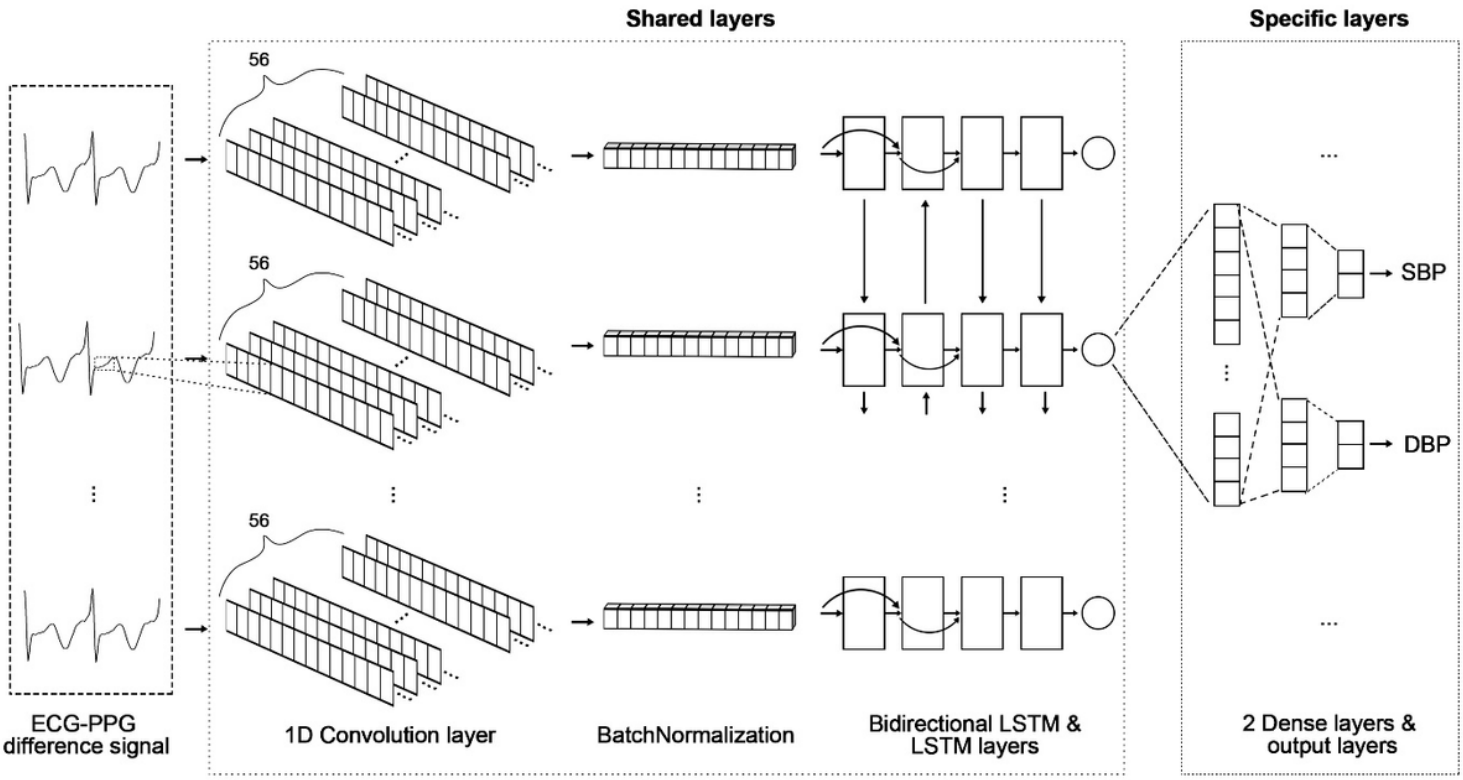

Figure 3

Proposed model architecture

Supplementary Files

This is a list of supplementary files associated with this preprint. Click to download.

- 0SupplementaryNIBP.pdf